

Chemical Turbulence and Line Defects Induced by Gradient Effects in a Three-Dimensional Reaction–Diffusion System

Chunxia Zhang,^{†,‡} Huimin Liao,^{†,‡} and Qi Ouyang^{*,†,‡,§}

Department of Physics, The Beijing-Hong Kong-Singapore Joint Center for Nonlinear and Complex Systems (PKU), and Center for Theoretical Biology, Peking University, Beijing 100871, P. R. China

Received: December 26, 2005; In Final Form: February 20, 2006

We report experimental observations of chemical turbulence and line defects in a three-dimensional (3-D) Belousov–Zhabotinsky (BZ) reaction–diffusion system. Transitions from spiral waves to 3-D chemical turbulence to line defects are observed. These transitions are caused by concentration gradients across the third dimension in the 3-D reaction medium, indicating the observed line defects have a 3-D structure. The line defects come out of the 3-D turbulent state, and become smooth with the increase of the control parameter. Simulation with the two-variable Oregonator model in the 3-D system reproduces similar line defects.

Introduction

Complex systems containing nonlinear dynamic elements can support various spatiotemporal patterns. Such systems are ubiquitous in nature and have been well studied in experiments. Among them, there exist a broad class of systems with complex periodic behavior, which have attracted a great deal of attention in recent years. A few years ago, Goryachev and Kapral^{1–4} revealed a set of new interesting phenomena in their numerical simulations with the three-variable Rössler reaction–diffusion system. They observed unusual spiral waves with multiple periods (period-2ⁿ), period-doubling bifurcations, and turbulent patterns in the oscillatory systems. This poses new challenges to scientists in a wide range of fields. Soon after, Park and Lee^{5–7} convincingly demonstrated the actual existence and systematically studied the properties of these complex patterns in a real laboratory system, the BZ reaction–diffusion system.

The most striking feature of these complex periodic patterns is the existence of “line defects”, across which the phase of local oscillation switches by a multiple of 2π . Taking period-2 (p-2) oscillatory media as an example, the local dynamics along the line defect, which is the boundary between regions of two p-2 oscillatory media, exhibits a p-1 oscillation. These line defects are actually a collection of spatial points at which the local oscillations are temporally different from those of the neighboring regions. A line defect is now believed to be a generic property of complex periodic patterns and has recently been well-studied on their bifurcation and dynamical behaviors. They can be either static or dynamic; they can be hidden behind the carrying waves^{5,6} as well as seen explicitly.⁸ Various forms of line defects have been observed both in experiments and in simulations, such as spiraling line defect,⁶ straight line defect,⁸ and sinusoidal-shaped line defect.⁷ Recent research has demonstrated that line defects can lose their stability by means of transverse instability.⁷

However, most of previous theoretical investigations are mainly based on 2-D systems. One should realize that a real

experimental system is actually a 3-D one with concentration gradients across the third (Z) direction. Earlier than Goryachev et al, Yoneyama et al have reported such defect lines in experiments on the spatially 3-D BZ reaction media.⁹ In a recent review paper by Park and Lee,¹⁰ the authors imply that these structures may, under certain conditions, be associated with dynamics caused by three-dimensional effects. Moreover, about 10 years ago, Winfree has suggested that 3-D media may possess special mechanisms of wave pattern, different in principle from the patterns in two-dimensional systems.¹¹ Following these suggestions, current researches on 3-D scroll waves have been yielding valuable achievements.^{12–14} This encourages us to seek the underlying mechanism of these complex patterns in 3-D space. Here, we report our experimental observations of travelling wave instability caused by 3-D effects of the system, and more importantly subsequent line defect structures coming out of the 3-D turbulent state. Numerical simulations with the Oregonator model are also performed on the basis of the 3-D system. This result shows similar line defect structures as observed in the experiments.

Experimental Setup

Our experiments are conducted in a spatially open reactor as described previously.¹⁵ The reaction medium is a thin porous glass disk (Vycor glass 7390, Corning), 0.4 mm in thickness and 25 mm in diameter, with an average porous size of 10 nm. The porous glass disk prevents any convection in the reaction medium so as to guarantee the necessary reaction–diffusion feature of the system. The opposite sides of the porous glass disk are respectively in contact with two reactant reservoirs (10 mL in volume for each), where the reactants are continuously refreshed by highly precise chemical pumps (Pharmacia, P-500) and kept homogeneous by magnetic stirring. Reagents of the Ferriin-catalyzed Belousov–Zhabotinsky (BZ) reaction are distributed in the two reservoirs in such a way that one (I) is kept in the reduced state and the other (II) is kept in the oxidized state. The reactants from both sides diffuse into the glass and meet within the reaction medium, where BZ reactions take place and sustained patterns occur.

As has been well documented in ref 16, there exist multiple concentration gradients across the reaction medium, so that the

* To whom correspondence should be addressed. E-mail: qi@pku.edu.cn.

[†] Department of Physics.

[‡] The Beijing-Hong Kong-Singapore Joint Center for Nonlinear and Complex Systems.

[§] Center for Theoretical Biology.

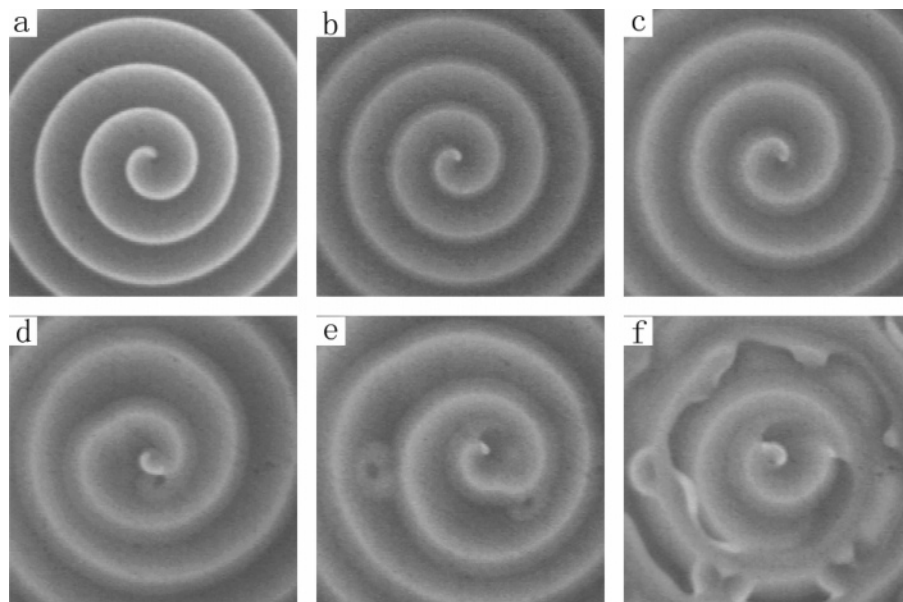


Figure 1. Experimental observations of the transition from a regular quasi-2-D pattern to 3-D chemical turbulence. $[\text{H}_2\text{SO}_4]^{\text{I}}$: (a) 0.3 M, a simple 2D spiral pattern; (b) 0.45 M, onset of 3-D structure of the pattern; (c) 0.5 M, deep into the 3-D system, the beginning of the separating and combing behavior of the tip area; (d, e, f) 0.55 M development of chemical turbulence.

system is actually a 3-D one. If well arranged, we can deliberately increase the thickness of the patterned layer so that the dynamics in the third direction (gradient direction) must be taken into consideration. In the experiment, we choose a regime in the space of control parameters such that with the increase of the control parameter $[\text{H}_2\text{SO}_4]^{\text{I}}$, the three-dimensional effect of the system becomes more pronounced step by step in the course of the experiment. According to the abundant experiments we have carried out, it can be deduced that the thickness of the patterned layer increases with the increase of $[\text{H}_2\text{SO}_4]^{\text{I}}$. As a result, the system changes from a quasi-2-D system to a 3-D one. In such a way we can study the gradient effects on the pattern formation and development of the system when it gradually transforms from a quasi-2-D medium to a 3-D medium. The concentrations of other reactants are kept fixed: $[\text{NaBrO}_3]^{\text{I,II}} = 0.2 \text{ M}$, $[\text{KBr}]^{\text{I}} = 60 \text{ mM}$, $[\text{CH}_2(\text{COOH})_2]^{\text{I}} = 0.6 \text{ M}$, $[\text{H}_2\text{SO}_4]^{\text{II}} = 0.2 \text{ M}$, and $[\text{Ferriin}]^{\text{II}} = 1.0 \text{ mM}$. The reaction temperature is $25 \pm 0.5 \text{ }^\circ\text{C}$, and the residence time of reactants in each side of the reservoir is fixed at 17 min.

As described in the previous work, the initial condition is chosen such that there is only one spiral tip residing in the center of the reaction medium. This condition can be achieved by using the same method as described in refs 16 and 17. Once a spiral is ready, we can study it by changing the control parameter step by step while fixing all the other conditions. Digital images of spatiotemporal patterns are generated by a CCD camera and stored in a computer for further analysis. Enough time (at least 1 h) is allowed before taking a record at every parameter point so that the system can relax to its asymptotic state.

Experimental Results

In the very beginning, we focus our attention on the system when the control parameter is relatively lower. At low $[\text{H}_2\text{SO}_4]^{\text{I}}$ (0.3 M), we observe a simple rotational spiral, as shown in Figure 1a. Under these experimental conditions, the spiral waves can be considered as entrained in the direction with gradients, so that no obvious 3-D structure is observed in this direction. When the control parameter is increased to 0.45 M, we observe a slight hint of a 3-D structure. As shown in Figure 1b, the

oxidized region (light region) of the waves becomes thicker and is not uniform. At this point, the system is gradually transforming from a quasi-2-D system to a quasi-3-D system. The tendency of the 3-D structure of the pattern becomes pronounced as the control parameter is continuously increased. Compared with Figure 1b, Figure 1c ($[\text{H}_2\text{SO}_4]^{\text{I}} = 0.5 \text{ M}$) shows that the tip area is no longer a point but a line. In terms of three-dimensional scroll waves, we call this line a filament. Because of the limitation of the experimental setup, we can only record the projection images along the gradient direction, so that the filament cannot be fully resolved. The tip filament seems inclined and periodically moving around. Viewing from the projection direction, we observe two spiral tips periodically separate and recombine. This phenomenon has been described in detail in our previous work.¹⁶ The 3-D structure of the pattern is obvious under these conditions, and the pattern is asymptotically stable. As the control parameter is increased further (0.55 M), transition to defect-mediated turbulence or spiral turbulence takes place. Figure 1d,e,f depicts the process of defect developing in the system. First, the filament stretches and bends. Soon the initial waves develop a bump in the neighboring region of the original filament [Figure 1d], resulting from the filament winding and touching the boundary of the reaction medium. After these first couple of defects appear, defects are continuously generated near the spiral filament and travel out [Figure 1e]. In the asymptotic state, the system is full of this type of defects, as shown in Figure 1e.

The observed spiral breakup scenario has previously been studied both in experiment¹⁶ and in simulation.¹⁴ Although there exist many candidates for the mechanism of this 3-D scroll wave breakup, such as negative tension of the spiral filament,^{12,13} the gradient effects of certain chemical reactants,¹⁶ spontaneous scroll ring creation, and their symmetry breaking,¹⁴ none of them can exclusively explain the whole process of this spiral wave instability. The situation in the experiments looks more complicated. At present, we may conclude that all the mechanisms mentioned above have certain contributions to this transition to spiral turbulence, but a quantitative description is still lacking. Further detailed investigations are still needed to interpret the whole course.

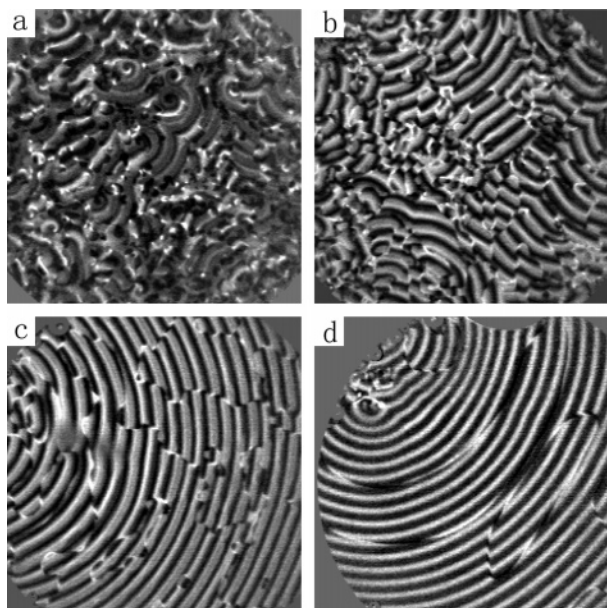


Figure 2. Snapshots of the pattern with the changing of $[\text{H}_2\text{SO}_4]^{\text{I}}$: (a) 0.7 M, highly disordered 3-D turbulent state; (b) 0.8 M, the emergence of wave segments with small line defects; (c) 0.9 M, a more ordered state with obvious line defects; (d) 1.2 M, line defects with smooth curvature.

If we further increase $[\text{H}_2\text{SO}_4]^{\text{I}}$ after the breakup of the waves, a new scenario will take place. Waves characterized by slow and erratic motion of line defects will emerge out of the sea of turbulence. When $[\text{H}_2\text{SO}_4]^{\text{I}}$ is increased to 0.7 M, the system goes deeper into the 3-D turbulent state. Figure 2a demonstrates a snapshot of this highly disordered state. As $[\text{H}_2\text{SO}_4]^{\text{I}}$ is further increased (0.8 M), small wave segments with irregular shapes constantly appear and decay. They crowd the whole reaction medium and distribute intricately within the highly complex turbulent sea [see Figure 2b]. Although in this state the system is still in disorder, we can see a slight hint of small pieces of line defects between two groups of wave segments, propagating along the same direction. When $[\text{H}_2\text{SO}_4]^{\text{I}}$ is further increased to 0.9 M, the system tends to self-organize into a more ordered state, as shown in Figure 2c. Waves propagating along a certain direction dominate and the characteristic scale of the line defects becomes longer compared with that in Figure 2b. But the shape of the line defects is still quite irregular, in contrast to the static line defects as previously described in ref 8. We notice that these crimped and irregular line defects are dynamic: they move slowly, erratically, and roughly along the direction of the wave propagating, and always disappear at the boundary of the reaction medium. The moving velocity of the line defects is about eight times slower than that of the carrying waves under this condition. With further increase of the control parameter, the degree of the winding of the line defects becomes lower, and the system seems to prefer line defects with smooth curvature. At the same time, the number of line defects within the reaction medium is much less than that of the state when $[\text{H}_2\text{SO}_4]^{\text{I}}$ is lower. Figure 2d gives a snapshot of this more ordered state of the system.

Line defects in our experiments can exhibit various forms. They can be associated with singular points (or defects) that coexist in the system, or terminate at the boundary of the reaction medium. They can also simply self-connect to form a closed loop. They may be perpendicular to the carrying wave train, substantially parallel to it, or located at an arbitrary angle with the waves. These observed line defects always travel along the propagating direction of the carrying wave train. They move

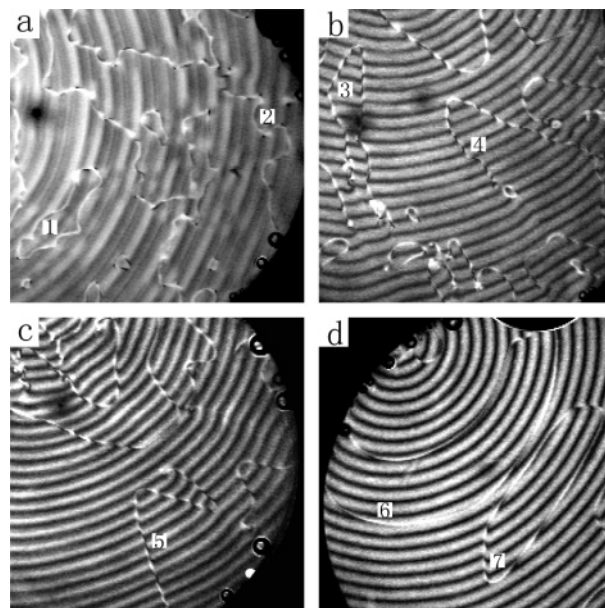


Figure 3. Various forms of line defects observed in the experiments: (a) 0.9, (b) 1.0, (c) 1.1, and (d) 1.2 M $[\text{H}_2\text{SO}_4]^{\text{I}}$. The number in the panels indicates different forms of line defects: 1, 7, line defects with a closed loop; 2, line defect with one end connecting to the boundary and the other to a defect; 3, line defect with both ends associating with defects; 4, line defect with an arbitrary angle to carrying waves; 5, line defect perpendicular to carrying waves; and 6, line defect substantially parallel to carrying waves with both ends terminating at the boundary.

very slowly, until they arrive at the boundary of the reaction medium and disappear. Figure 3 gives examples of various forms of line defects observed in the experiments. The pictures are obtained by using the processing method provided in ref 7.

Simulation

From the experimental observations, we are quite certain that the line defects are closely related to the 3-D effects of the system. To understand more clearly the spatiotemporal structure of these line defects and the role the 3-D effect plays in the system, we conducted 3-D simulations with the two-variable reduced Oregonator model, which was extensively studied by Tyson and Fife.¹⁸

$$\frac{\partial u}{\partial t} = \frac{1}{\epsilon} \left(Au - u^2 + fBv \frac{qA - u}{qA + u} \right) + D_u \nabla^2 u \quad (1)$$

$$\frac{\partial v}{\partial t} = Au - Bv + D_v \nabla^2 v \quad (2)$$

The variables u and v describe the concentrations of the activator HBrO_2 and the inhibitor catalyst ferriin, respectively; A , B denote $[\text{BrO}_3^-] \cdot [\text{H}^+]$ and the total concentration of the organic substrate, respectively; f , ϵ , and q are parameters; D_u and D_v are the diffusion coefficients of the two variables; and ∇^2 is a three-dimensional Laplacian operator ($\partial^2/\partial x^2 + \partial^2/\partial y^2 + \partial^2/\partial z^2$). We make the original model to be able to account for the gradients across the reaction medium.¹⁹ To simulate this 3-D effect, we introduce the gradients of A , B , and f along the Z direction, simply varying them linearly between the bottommost surface and the topmost surface. The calculations are performed on a $256 \times 256 \times 15$ grid, using 19-point approximation for the Laplacian operation in 3-D,²⁰ imposing the no-flux boundary condition with time step $dt = 0.01$ and space step $h_x = h_y = h_z = 0.01$. In our simulation, we use the value of A at the topmost

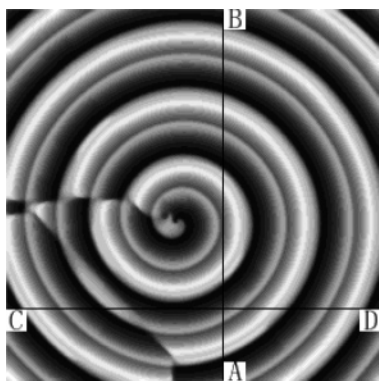


Figure 4. 2-D projection of waves with explicit line defects in the two-variable 3-D simulation. Parameter A at the topmost surface is 0.09.

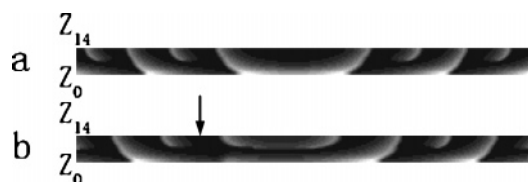


Figure 5. Waves in the vertical plane with Z_0 and Z_{14} denoting the bottommost surface and the topmost surface, respectively: (a) along AB in Figure 4 (Y – Z plane); and (b) along CD in Figure 4 (X – Z plane), the arrow indicates the location of the line defect.

surface as the control parameter. Other parameters are fixed: $D_u = 5 \times 10^{-5}$; $D_v = 3 \times 10^{-5}$; $\epsilon = 0.01$; $q = 2 \times 10^{-4}$; bottommost surface $f = 2.5$, $B = 0.1$, and $A = 0.08$; and topmost surface $f = 1.5$ and $B = 0.6$.

Figure 4 shows a typical result of our simulation in the projection direction of the X – Y plane. We can see an explicit irregular line defect that connects the spiral tip at one end and the boundary at the other end. This line defect is similar to those observed in the experiments. To demonstrate what is happening for the system in the vertical plane, we record the information of the system along the solid lines AB and CD as denoted in Figure 4. They correspond to Figure 5a (Y – Z plane) and Figure 5b (X – Z plane), respectively. Due to the concentration gradients along the Z direction, different layers of the system have a different dispersion relationship, which determines the period and the wavelength of the spiral pattern. If we decouple the relationship between each layer in the gradient direction, waves in the upper part of the system will have periods relatively smaller than those in the lower part of the system. Diffusive coupling between different layers in the gradient direction reorganizes patterns in the system. To acquire a balanced state between different layers, the system has to adjust along the vertical Z direction. As a result, waves along this direction become inclined instead of vertical. More importantly, for every other wave, it stops propagating in the middle so that the system is composed of two kinds of waves, longer waves and shorter waves. They alternatively arrange themselves across the reaction medium and propagate out, as shown in Figure 5. Reflected on the X – Y projection plane, the system exhibits waves with nonuniform width and gray level. Line defects appear where the longer wave and the shorter wave switch positions, as is clearly demonstrated in Figure 4. When there are no line defects in the local region, waves in the vertical plane align in a manner that longer waves and shorter waves appear alternately, as shown in Figure 5a; if line defects appear, this orderly alignment of the local region will be disturbed. As demonstrated in Figure 5b, two shorter waves exist adjacently across the line defect indicated by the arrow. This line defect is qualitatively different

from those in 2-D systems, where line defects are caused by the period-doubling bifurcation mechanism.

It is worth of noting that our simulations serve only to qualitatively understand the underlying line defect mechanism of the experimental observations. The Oregonator model is just a simplified theoretical model; it cannot accurately describe the actual experimentally observed phenomena. Many disagreements exist between experimental results and numerical simulations. For example, in the simulation the initial waves do not evolve into the turbulent state, line defects come out of ordered waves instead of turbulent states, and compared with the situation in the experiment, there are few forms of line defects. Despite all these disagreements, the result of the simulation can still account for the phenomena in some respects. Further theoretical analysis and a more accurate model need to be found to finally resolve the problem.

Conclusion

We reported a special phenomenon regarding line defects in the BZ reaction–diffusion system. In contrast with previous studies where the investigations on line defects are mostly conducted in two-dimensional systems, our observation provides convincing evidence that the line defects in our experiments have a 3-D structure. First, the boundary conditions at two opposite sides of the reaction medium are not identical and concentration gradients exist across the medium, so that to some extent, it is necessary to consider the gradient effects along this direction. Second, referring to the whole course of this phenomenon, experimental evidence indicates that there is a transition of the system from quasi-2-D structure to 3-D structure. The line defects come out of the 3-D scroll-like wave instability, so that they must have a 3-D structure. Third, our 3-D simulations reproduce line defects similar to those observed in the experiments. We can also deduce that the line defect in this experiment is a result of the dispersion relation differences between different layers, which are caused by the concentration gradients in the 3-D system. This mechanism is essentially different from those studied in 2-D systems, where the wavelength-doubled phenomenon is caused by the period-doubling bifurcation.

In the pioneering work of Yoneyama et al.⁹ the authors clearly demonstrated the existence of the line defects in a 3-D system, by studying pattern formation on the surface and inside the solution, respectively. They conducted the experiments in a closed system with a gradient of [oxygen]. In contrast, our experiments were conducted in an opening system with multiple concentration gradients of reagents. With our experimental equipment, we can study the asymptotic behavior of the system and the development of the line defects with the changing of the control parameters. Another point is that in our experiments, the line defects come out of the 3-D turbulent state, which is different from Yoneyama's work.

As discussed in the previous sections, there are many disagreements between experimental results and numerical simulations. We believe that the 3-D experimental system is rather complicated, and the phenomena observed can never be explained only by one or two factors. For example, the scroll wave breakup observed in our experiments may be associated with negative tension instability,¹² because in the simulation we can also see the tip area of the waves has the same separating and combining behavior as observed in the experiments. But this does not rule out the mechanism of spontaneous scroll ring creation and their symmetry breaking.¹⁴ Further experiments on the same system may help to figure out the full picture. In any

case, the dynamical properties of the line defects are abundant and complicated. There is still much effort needed to elucidate clearly the line defects in the 3-D system.

Acknowledgment. We thank X. Cheng, C. Wang, and S. Wang for helpful discussion. This work is supported by the Chinese Natural Science Foundation and the Department of Science of Technology in China.

References and Notes

- (1) Goryachev, A.; Kapral, R. *Phys. Rev. Lett.* **1996**, 76, 1619.
- (2) Goryachev, A.; Kapral, R. *Phys. Rev. E* **1996**, 54, 5469.
- (3) Goryachev, A.; Chaté, H.; Kapral, R. *Phys. Rev. Lett.* **1998**, 80, 873.
- (4) Goryachev, A.; Chaté, H.; Kapral, R. *Phys. Rev. Lett.* **1999**, 83, 1878.
- (5) Park, J. S.; Lee, K. J. *Phys. Rev. Lett.* **1999**, 83, 5393.
- (6) Park, J. S.; Lee, K. J. *Phys. Rev. Lett.* **2002**, 88, 224501.
- (7) Park, J. S.; Lee, K. J. *Phys. Rev. Lett.* **2004**, 93, 098302.
- (8) Guo, H. Y.; Wang, H. L.; Ouyang, Q. *Phys. Rev. E* **2004**, 69, 056203.
- (9) Yoneyama, M.; Fujii, A.; Maeda, S. *J. Am. Chem. Soc.* **1995**, 117, 8188.
- (10) Park, J. S.; Lee, K. J. *Phys. Rev. E*. In press.
- (11) Winfree, A. T. *Science* **1994**, 266, 1003.
- (12) Alonso, S.; Sagués, F.; Mikhailov, A. S. *Science* **2003**, 299, 1722.
- (13) Alonso, S.; Kähler, R.; Mikhailov, A. S.; Sagués, F. *Phys. Rev. E* **2004**, 70, 056201.
- (14) Wang C.; Wang, S.; Zhang, C. X.; Ouyang Q. *Phys. Rev. E* **2005**, 72, 066207.
- (15) Ouyang, Q.; Swinney, H. L. *Chaos* **1991**, 1, 411.
- (16) Zhang, C. X.; Zhang, H.; Ouyang, Q.; Hu, B. B.; Guraratne, G. H. *Phys. Rev. E* **2003**, 68, 036202.
- (17) Ouyang, Q.; Swinney, H. L.; Li, G. *Phys. Rev. Lett.* **2000**, 84, 1047.
- (18) Tyson, J. J.; Fife, P. C. *J. Chem. Phys.* **1980**, 73, 2224.
- (19) Vasquez, D. A.; Horsthemke, W.; McCarty, P. *J. Chem. Phys.* **1991**, 94, 3829.
- (20) Dowle, M.; Mantel, R. M.; Barkley, D. *Int. J. Bifurcation Chaos* **1997**, 7, 2529.